Materials and Design 31 (2010) 1497–1507

Contents lists available at ScienceDirect

Materials and Design

journal homepage: www.elsevier.com/locate/matdes

# Numerical simulation of linear friction welding of titanium alloy: Effects of processing parameters

Wen-Ya Li *, Tiejun Ma, Jinglong Li

*Shaanxi Key Laboratory of Friction Welding Technologies, Northwestern Polytechnical University, Xi'an 710072, Shaanxi, PR China*

ARTICLE INFO

*Article history:*
Received 12 March 2009
Accepted 15 August 2009
Available online 19 August 2009

*Keywords:*
Linear friction welding
Explicit finite element analysis
Titanium alloy
Temperature field
Axial shortening
Processing parameters

ABSTRACT

Numerical modeling of linear friction welding (LFW) of TC4 titanium alloy was conducted using ABAQUS/Explicit with a 2D model. The coupled thermo-mechanical analysis was performed with the Johnson–Cook material model. The effects of processing parameters on the temperature evolution and axial shortening of LFW joints were numerically investigated. It is shown that the temperature at the interface can first increase quickly to about 1000 °C within 1 s, then increases slowly, and finally tends to become uniform across the interface under certain processing conditions. The temperature gradient across the joint from the interface is very high during the friction process. Consequently, significant axial shortening and fast formation of flash start to happen as the interface temperature becomes more uniform. During cooling, the interface temperature decreases steeply at a rate of several hundred degrees per second because of the fast heat conduction to the cold end of the specimen. The temperature distribution appears to be uniform in the joint after about 30 s. At a higher oscillation frequency, the interface temperature rises more quickly and the axial dimension shortens more and at a faster rate. The same phenomena are observed for the amplitude and friction pressure. The effects of these three factors can be integrated into one parameter of heat input. The axial shortening increases with increasing heat input almost linearly as the heat input exceeds a critical value.



## 1. Introduction

LFW is a process that involves frictional heating of the workpiece faying surfaces by reciprocal (linear) motion as schematically shown in Fig. 1a. This process effectively extends the utility of friction welding beyond rotational welding to include the joining of noncircular workpieces. In addition, similar to other friction welding (FW) techniques, LFW offers a means of joining free from melting and re-solidification processes and allows for the formation of a narrow heat affected zone (HAZ) due to an extremely localized band in which heat is generated. This makes the process very attractive for joining difficult to weld, high performance materials and dissimilar alloys. LFW is observed to have four distinct phases (Fig. 1b), i.e. the initial phase, the transition phase, the equilibrium phase, and the deceleration (or forging) phase [1–3]. During LFW process, frictional heat is generated and results in continued plasticization of the interfacial region between the components. Furthermore, the plastically deformed material is displaced toward the weld edges to form a flash (upset metal). Once sufficient plasticization has occurred, a forging force is applied to produce a consolidated joint seam with limited thermo-mechanically affected zone (TMAZ) and HAZ. Therefore, achieving a successful friction weld the process relies upon introducing some plasticity into both parts despite the potentially widely differing ability of the materials to plastically deform under the given processing conditions.

Although available for almost twenty years, LFW has only found industrial application in aircraft engine manufacture, in part due to the high cost of the welding machines. It has proved to be an ideal process for joining turbine blades to disks where the high value-added cost of the components justifies the cost of a LFW machine. This approach is more cost-effective than machining blade/disc (blisks) assemblies from solid billets. On the material's side, LFW has been applied successfully to a range of materials including titanium alloys [1–10], superalloys [11], steel [12,13], intermetallic materials, aluminum, nickel, copper, and even dissimilar material combinations with the greatest emphasis on aircraft engine alloys [14]. The MTU group is presently manufacturing blisks for PW6000, EJ200, TP400, F119 engines with the LFW process [4,5]. Although aeroengine companies are currently investing developing more about LFW, only a limited number of publications can be found in the open literature.

Previous studies showed that the sound welds (e.g., Ti64 [1,8–10,15], Ti6242 [7], Ti6246 [5,6], medium carbon steel [13]) with the refined microstructure could be obtained by LFW. The welds presented much higher [5,7–9] or lower [13] hardness, and

* Corresponding author. Address: School of Materials Science and Engineering, Northwestern Polytechnical University, Xi'an 710072, PR China. Tel.: +86 29 88495226; fax: +86 29 88491426.
*E-mail address:* liwy@nwpu.edu.cn (W.-Y. Li).

0261-3069/$ - see front matter 
doi:10.1016/j.matdes.2009.08.023

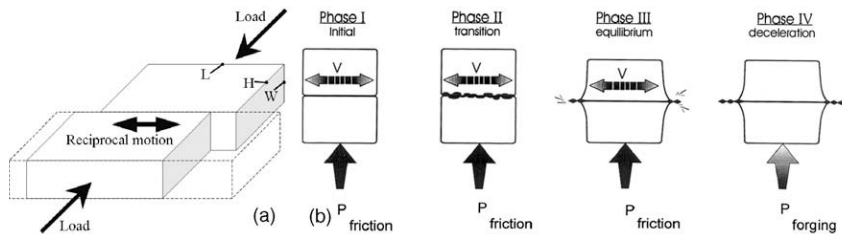


**Fig. 1.** Schematic illustration of the LFW process (a) and its stages (b) [1–3].

comparable or slightly better tensile properties [8,9,13] than the parent owing to the refined structure. However, their fracture properties (e.g., impact toughness) are difficult to predict because the microstructure produced in the weld region is very heterogeneous, and even more difficult when two different base materials are welded together [1,5,15]. In addition, the special heating and cooling processes in LFW make it complex to reveal the microstructure evolution in the joints. Thus, it is very difficult to investigate simply by experimental observation due to the complicated coupling of thermal and mechanical effects, such as the variation of thermo-physical properties with temperature and the change of mechanical properties with deformation conditions (e.g., temperature and strain rate). As such, numerical analysis using advanced computational tools can play an important role in providing insight to the complex LFW process.

In the pioneer work by Vairis and Frost [1–3], the LFW process was analyzed and modeled with the temperature evolution and material flow of Ti64 joints. They first analyzed the temperature evolution based on a 1D transient heat conduction model, and then discussed the effect of the exothermic reaction of titanium with oxygen during the extrusion phase [3]. The predicted temperature data was to some extent consistent with the experiment and the exothermic reaction is not an important contribution to the temperature rise in the flash or the neighboring specimen [3]. They also developed an analytical model to predict the strain rates based on the macroscopic examination of the flash and axial shortening data from experiments [2]. In a recent report by Tao et al. [16], thermo-mechanical coupled analysis of LFW Ti64 was conducted by using the DEFORM software. The computed temperature data and axial shortening of joint were comparable to the experimental result [16]. In sum, much work is needed in modeling the LFW process to reveal more detailed nature.

In this study, a new simulation method was developed with a 2D model based on the commercial software ABAQUS/Explicit (Ver 6.7). The coupled thermo-mechanical explicit analysis was conducted by using the Johnson–Cook material model which takes into account the effects of strain hardening, strain rate strengthening and temperature softening. The changes of material's thermal properties and friction coefficient with temperature were also considered. Both the frictional heat and plastic deformation dissipated heat were adopted in the model. The effects of processing parameters on the temperature evolution and axial shortening of LFW joints were numerically investigated.

## 2. Numerical method

### 2.1. 2D model

According to the characteristics of LFW, it is very difficult to meet satisfactorily the requirements for the computer if the model was built based on the true specimen size. Therefore, a 1/4 model was used as shown in Fig. 2a. This 3D model was firstly simplified to one workpiece with a rigid surface, and then 1/2 part along the oscillation direction according to the feature of movement and the symmetric deformation of a similar joint. As indicated by Vairis and Frost [3], the process model of LFW of similar metals can be reduced to half of the original model size. This is because of the symmetric deformation of the joint based on the experimental observation [1,8,9]. Although frictional heat is generated between deformable and rigid surfaces, only 50% of frictional heat is designated to the deformable workpiece. Although some asymmetric deformation in the flash could be observed in the real joint, the focused temperature field along the joint is reasonable and consistent with the experiment. In addition, the rigid surface may

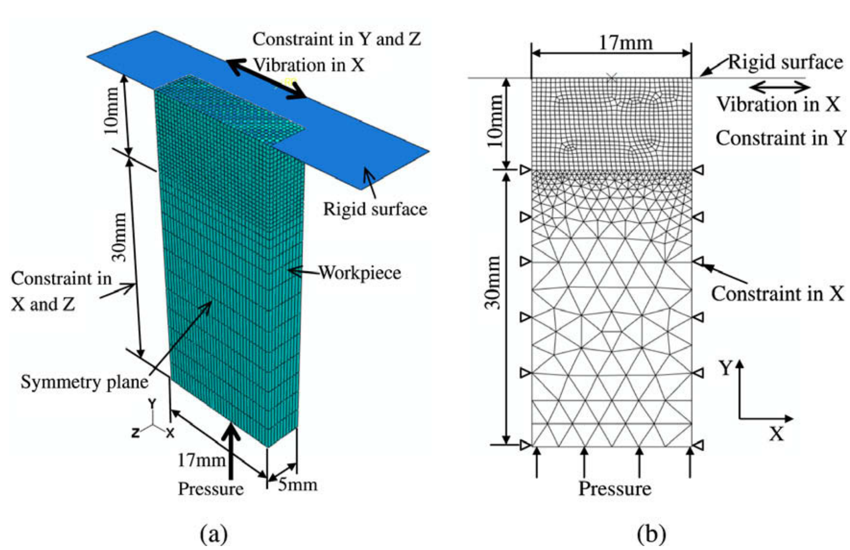


**Fig. 2.** (a) 3D and (b) 2D models with boundary conditions and meshing arrangement.

influence the interface behavior compared to two deformable workpieces. But the local interface is also not the focus of this study. Therefore, a rigid surface is assumed in our model to reduce the computation time. However, our preliminary study showed that the above 3D model was still not satisfactory owing to the strict limitation in the time increment for the explicit procedure in ABAQUS [17]. It takes several days or more with the present computer. Therefore, a 2D model as shown in Fig. 2b was developed to further reduce the computation time. This 2D model takes several hours compared to several days in the 3D model. This 2D model is a slice along the oscillation direction from the middle of the 3D model. The preliminary results have proved that this 2D model is very comparable to the 3D model. The specimen has a width of 17 mm and height of 40 mm. For meshing and adding constraints, the specimen was partitioned into two regions, where the upper 10 mm region has a meshing size of 0.5 mm and the lower 30 mm region has a gradually changing meshing size as shown in Fig. 2b. The meshing was conducted by using the 4-node quad element with coupled displacement and temperature, reduced integration and hourglass control, while the other elements are triangular as shown in Fig. 2b. Therefore, the numbers of elements are significantly reduced.

### 2.2. Boundary conditions and simulation settings

As shown in Fig. 2b, the external boundary of the lower 30 mm region was only permitted to move in the *Y* direction and constrained in the *X* direction. A given pressure was applied at the bottom surface of the specimen in the *Y* direction. The rigid surface on the top surface was solely permitted to move in the *X* direction in a sinusoidal mode with a given amplitude and frequency. Each sine cycle was divided into 40 parts along the time axis and the corresponding amplitudes were input to the code for calculation.

The interaction between the workpiece and rigid surface was implemented by using the surface-to-surface contact (explicit) formulation available in ABAQUS. The friction coefficient at the interface was varied with the temperature as shown in Fig. 3. According to the literature [18], the friction coefficient is affected by many factors, such as interface pressure, temperature and slip speed. However, due to the lack of available data for the materials and friction conditions in the literature, the values in this study are somewhat subjective but in a reasonable range [3,18]. In addition, 90% of plastic work is dissipated as heat based on the commonly used empirical assumption [19]. The available dynamic-temperature–displacement-explicit procedure (coupled thermal–mechanical analysis) in ABAQUS [17] was used, which takes into consideration heat conduction within the specimen.

It is well known that when the elements are excessively distorted with the Lagrangian algorithm under the conditions of large strain and high strain rate, it may lead to unreasonable results or premature termination of the program. One measure to cope with this problem in ABAQUS is Arbitrary Lagrangian Eulerian (ALE) adaptive mesh controls [17]. This ALE adaptive meshing was used with a remeshing frequency of 1 and remeshing sweeps of 50 per increment.

The initial temperature of the specimen was set at the room temperature (25 °C). As the first approximation, a heat transfer coefficient of 100 W/(m$^2$ K) for convection was adopted for the lat-

**Table 1**
The processing parameters studied.

| Parameter | Value |
|---|---|
| Oscillation frequency (Hz) | 25, 35, 45 |
| Amplitude (mm) | 2.5, 3.5, 4.5 |
| Friction pressure (MPa) | 20, 40, 60 |

**Table 2**
Properties of TC4 used in simulations [21,22].

| | |
|---|---|
| Density (kg/m$^3$) | 4430 |
| Young's modulus (GPa) | 114 |
| Poisson's ratio | 0.34 |
| Johnson–Cook model | |
| $A$ (MPa) | 418.4 |
| $B$ (MPa) | 394.4 |
| $n$ | 0.47 |
| C | 0.035 |
| $m$ | 1.0 |
| $T_r$ (°C) | 25 |
| $T_m$ (°C) | 1660, 1000 [23] |
| $\dot{\varepsilon}_o$ | 1 |
| Conductivity (W/m K) | See Fig. 4 |
| Specific heat (J/kg K) | See Fig. 5 |

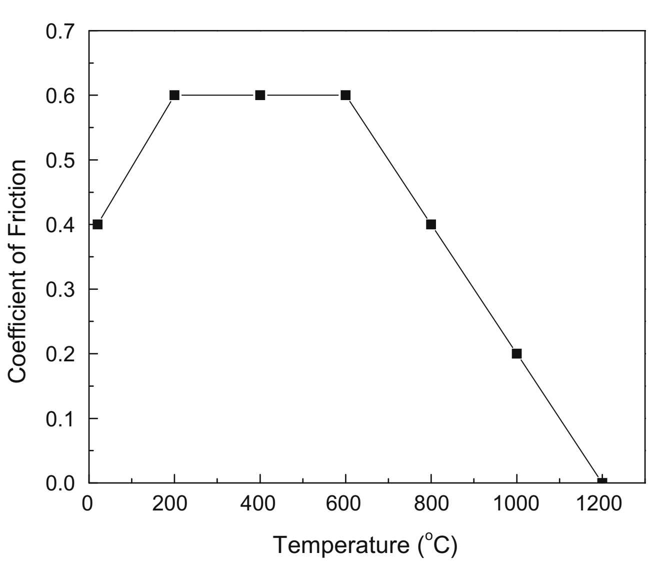


**Fig. 3.** Change of interface friction coefficient with temperature used in simulations.

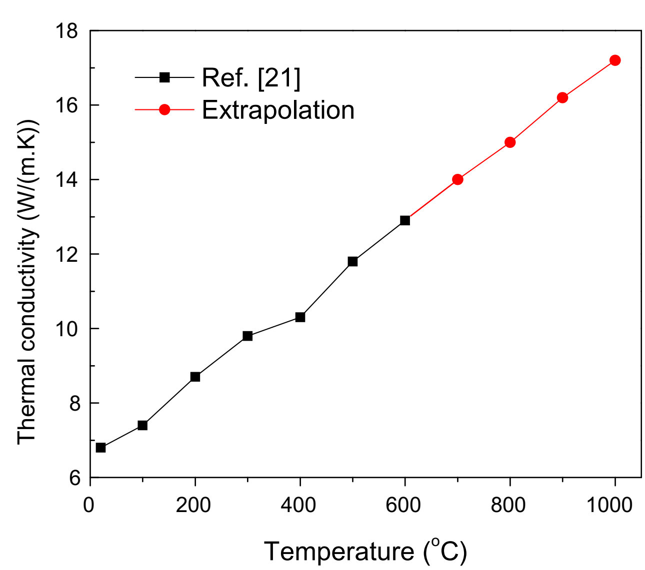


**Fig. 4.** Change of thermal conductivity with temperature.

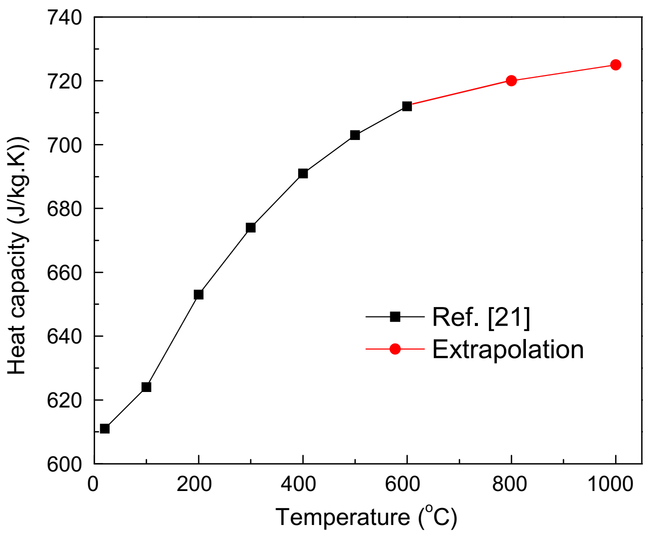


**Fig. 5.** Change of heat capacity with temperature.

eral surfaces according to the literature [3]. In this current study, we focus on the processing factors such as oscillation frequency, amplitude and friction pressure. The values of these parameters studied are listed in Table 1 and they are based on the LFW machine in our university.

### 2.3. Material properties

TC4 titanium alloy (Ti–6Al–4 V) was used in simulations. The properties of TC4 used in the simulations are listed in Table 2 that are obtained from the literatures [20–22]. The variation of thermal conductivity and heat capacity with temperature is shown in Figs. 4 and 5, respectively [21]. Part of the data at the temperature higher than 600 °C was extrapolated according to data from Ref. [20].

For mechanical properties, the material's deformation was described by the Johnson and Cook (JC) plasticity model, which accounts for strain hardening, strain rate hardening and thermal softening effects. The stresses are expressed according to the Von Mises plasticity model. The flow stress ($\sigma$) of material is expressed as follows [17]:

$$\sigma = (A + B\varepsilon_p^n)(1 + C\ln(\dot{\varepsilon}^*))(1 - (T^*)^m) \tag{1}$$

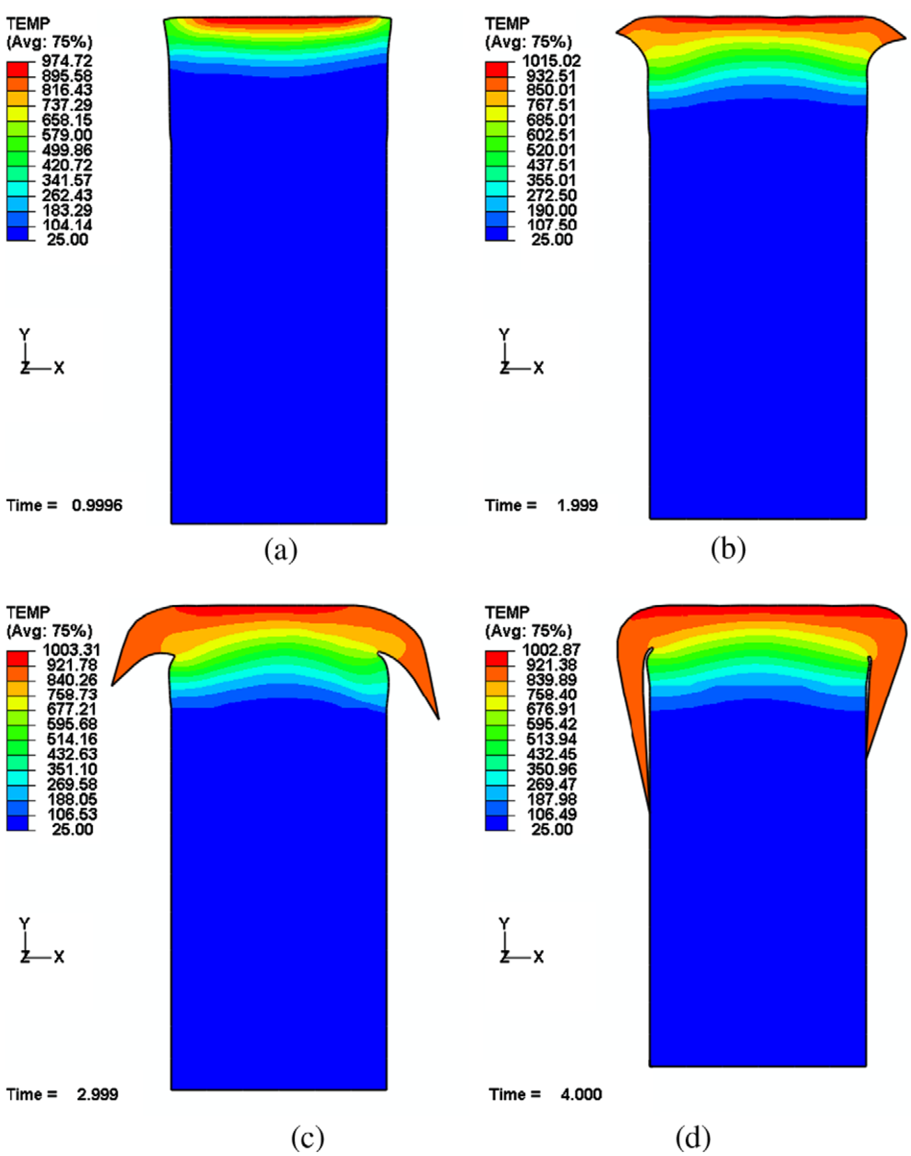


**Fig. 6.** Temperature contours in the specimen at different friction times: (a) 1 s, (b) 2 s, (c) 3 s and (d) 4 s.

where $A$, $B$, $n$, $C$, $m$ are material constants, $\varepsilon_p$ is the effective plastic strain (PEEQ), $\dot{\varepsilon}^*$ is the effective plastic strain rate normalized with respect to a reference strain rate $(\dot{\varepsilon}_p/\dot{\varepsilon}_0)$. $T^*$ is a homologous temperature defined as [17].

$$T^* = \begin{cases} 0 & \text{for } T < T_r \\ (T - T_r)/(T_m - T_r) & \text{for } T_r \leqslant T \leqslant T_m \\ 1 & \text{for } T > T_m \end{cases} \quad (2)$$

where $T_m$ is the melting point and $T_r$ is the reference or transition temperature. It is worth noting that the melting point used early by Johnson and Cook is the thermo-dynamic melting point which is about 1660 °C for TC4. However, according the previous investigation [23], TC4 will lose its resistance to plastic deformation at a temperature far below the thermo-dynamic melting point. Therefore, a lower melting point was used for the calculation of residual stresses in the welds [24]. Consequently, in this study, a temperature of 1000 °C was adopted for the melting point according to the yield strengths of TC4 against the temperature [23].

## 3. Results

### 3.1. Typical features of temperature evolution

In this representative case, the oscillation frequency, amplitude and friction pressure are 35 Hz, 3.5 mm and 40 MPa, respectively, based on the preliminary experiments. Fig. 6 shows the temperature distributions in the specimen at different friction times. It is seen that the temperature at the interface is quickly increased to above 970 °C at 1 s (Fig. 6a, also see Fig. 7), but the high temperature is only limited in the center region. The temperature is less than 600 °C at the margin (Fig. 6a). Therefore, the joint has been deformed a little with a small axial shortening (Fig. 8). No obvious flash has been formed at this moment. With further increase of friction time, the interface temperature increased further but slowly to near 1000 °C at 2 s (Fig. 6b) which is higher than 980 ± 10 °C for $\alpha + \beta \leftrightarrow \beta$ temperature of TC4. Vairis et al. [3] and Wanjara et al. [8] also indicated the peak interface temperature exceeding the $\beta$ transus temperature. The interface temperature has been uniform and the flash is observed. But the axial shortening is only around 0.7 mm at 2 s. While at 3 s (Fig. 6c), the interface temperature changed little, but more flash is formed and the axial shortening is about 2 mm. These results suggest that the LFW process has been in the so-called quasi-stable state. At 4 s (Fig. 6d), the interface temperature also changed little, but the axial shortening increased almost linearly and quickly to about 3.8 mm (Fig. 8). Due to the oscillation, the temperature curve also showed some vibration (Fig. 7). In addition, the temperature gradient from the interface in the joint is very large during the LFW process as shown in Fig. 6. Moreover, owing to poor thermal conductivity of TC4, the thickness of the high temperature zone (>900 °C) is only about 1 mm during the LFW process. The HAZ is also limited within 2 mm, which is consistent with the observed microstructure evolution [8,9].

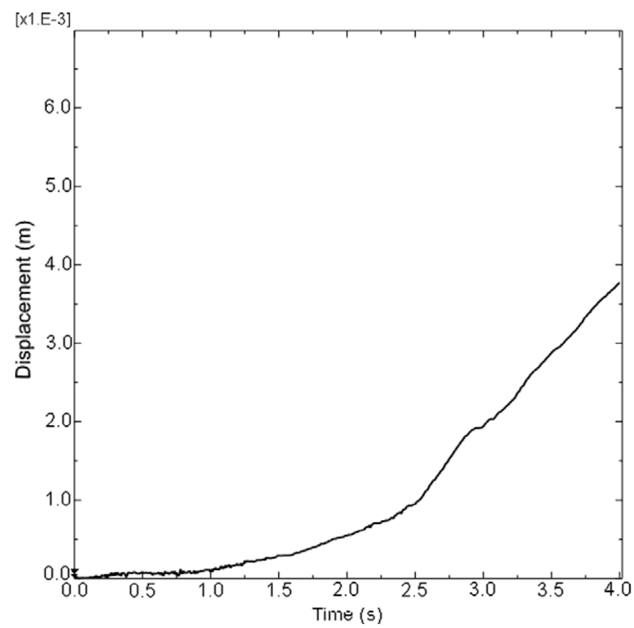


**Fig. 8.** Change of axial shortening with friction time.

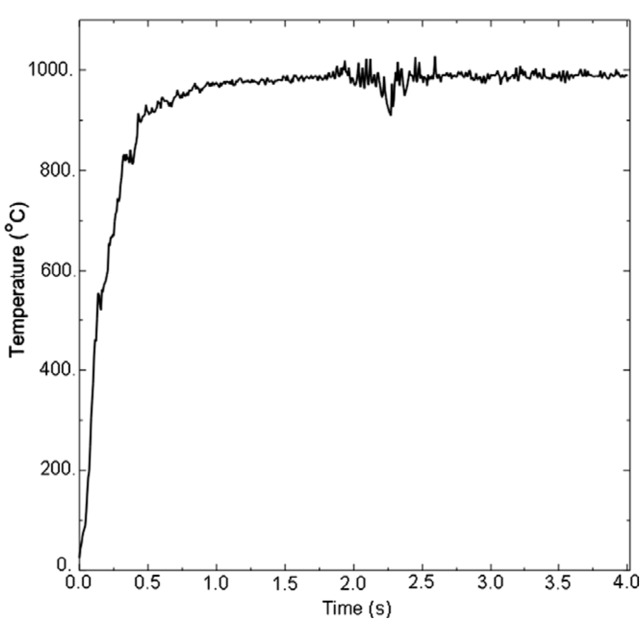


**Fig. 7.** Change of temperature of the central element at the interface with friction time.

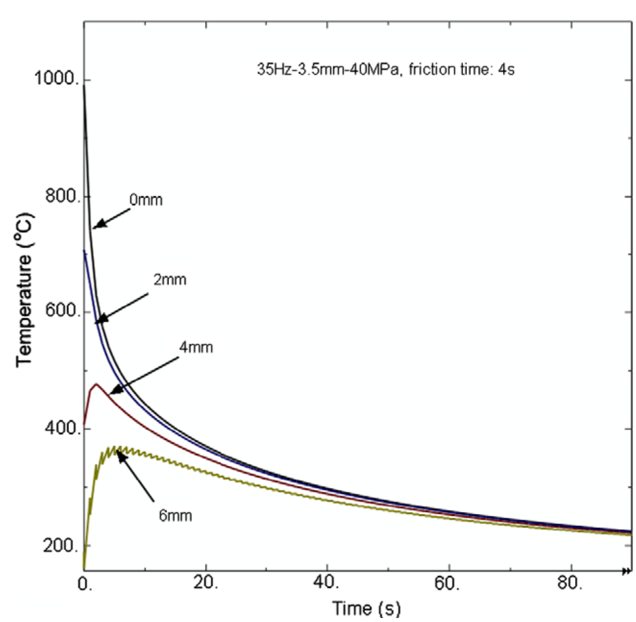


**Fig. 9.** Changes of temperatures at different distances from the interface center with cooling time.

It is worth noting that the flash is obviously curved (Fig. 6d). This phenomenon is not realistic, which is because the adhesion could not be considered in the simulation. Nevertheless, the temperature distribution is very reasonable.

In order to investigate the cooling process in a LFW joint, the 2D model used in the explicit procedure was adjusted to the implicit procedure with the coupled temperature–displacement (transient). The results obtained in the previous explicit procedure, i.e., at 4 s, were introduced as the initial conditions of the implicit procedure. The cooling time is 90 s.

Fig. 9 shows the temperature variations at different distances from the center of the interface with the cooling time. It is clearly seen that the cooling rate is very fast at the interface due to the heat conduction to the cold end of specimen. The interface temperature (0 mm) could be decreased from about 990 °C to 540 °C within 5 s, and cooled to 330 °C at about 30 s. The initial cooling rate is around 250 °C/s. In addition, the cooling rates at different positions vary. At the distance of 2 mm from the interface, the temperature is also cooled rapidly to a low temperature at about 30 s. While at the positions of 4 mm and 6 mm, the temperatures increased within a first few seconds, and then decreased quickly to the temperature close to the interface at about 30 s. These observations mean the heat conduction takes an important role in the joint cooling process. Finally, the temperature tends to be uniform within the specimen, which can be seen clearly from Fig. 10. From then on (after 30 s), the entire specimen will cool down all together mainly through the heat convection to the ambient. Furthermore, the result in Fig. 10 also reveals that the HAZ is limited within 2 mm from the interface for TC4 under the current processing parameters.

If the heating and cooling processes are plotted together as shown in Fig. 11, one can see the fast heating and cooling nature of the LFW process. This fast temperature variation has significant influence on the joint microstructure and properties [1,5,7–11,13].

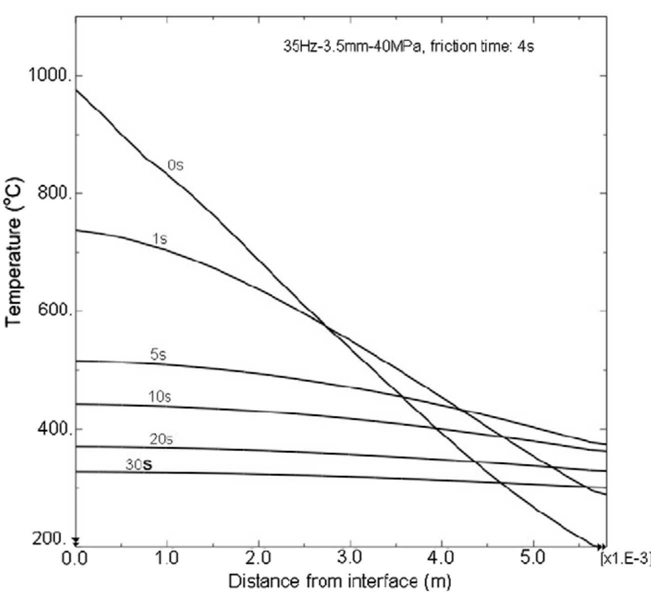


**Fig. 10.** Distributions of temperature along the distance from the interface center at different cooling times.

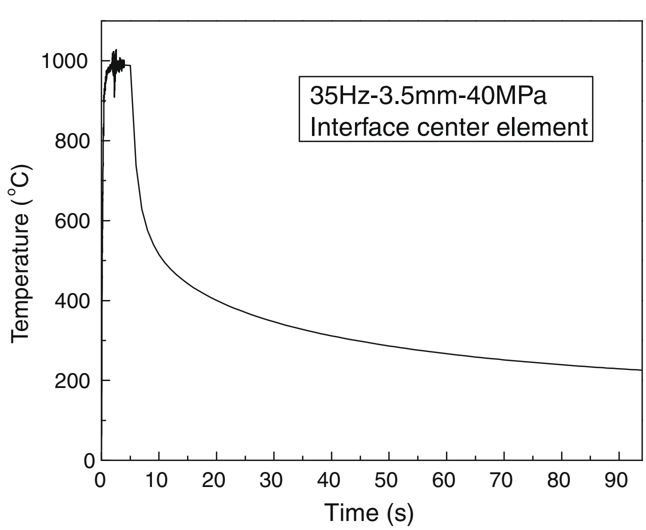


**Fig. 11.** The whole welding thermal cycle of the central element at the interface.

### 3.2. Effect of oscillation frequency

As experimentally indicated by Wanjara and Jahazi [8], the increase of frequency could significantly reduce the welding time. Vairis and Frost [1] also showed that the increase of frequency could increase the specific power input and decrease the required amplitude to obtain a good weld. The mass expelled per cycle also increased with the increase of frequency [1]. Based on the results in Section 3.1, the oscillation frequency is changed to 25 Hz and 45 Hz with the constant amplitude of 3.5 mm and friction pressure of 40 MPa. The calculated results are illustrated in Figs. 12 and 13. Compared to the results obtained under the frequency of 35 Hz (Fig. 6), the temperature distributions and evolutions present the same tendency. Although the temperature at the interface center with 25 Hz reached about 1000 °C at 1.5 s (Fig. 13a) and tended to be uniform at 4 s (Fig. 12a), the total unilateral axial shortening of the joint is about 1.1 mm (Fig. 13b) and just a little flash has been formed. It is found that the temperature at the interface increased relatively slowly and the margin temperature is too low to obtain an appropriate temperature filed earlier. This is because the heat input under low frequency is not enough to heat the interface zone. Therefore, a long friction time is necessary to deform the joint. But this situation will lead to severe oxidizing of the interface because it is not closed by the extruded materials, thus a lowered impact strength [1].

On the contrary, under the frequency of 45 Hz, the temperature at the interface increased more quickly and tends to be uniform across the interface earlier. It can reach about 1000 °C at 0.5 s (Fig. 13a). At 4 s (Fig. 12b), more materials have been extruded to form the obvious flash at a faster rate. The unilateral axial shortening under 45 Hz could be as large as 6.4 mm (Fig. 13b). This is because the heat input under 45 Hz is high enough to make the joint deform extensively at an earlier stage. At the same time, the thickness of high temperature zone is thinner with increasing frequency (Figs. 6d and 12) due to the faster extrusion of interface materials. It is considered that, under this condition, the entire interface could be enveloped by the flash earlier and a high-quality weld is expected.

According to these numerical results, it is expected that higher frequency would be more effective and efficient. However, for the sake of precision control of the joint dimensions, this condition may not be ideal due to the fast deformation rate, which will increase the difficulty in controlling the axial shortening. In addition, normal LFW machine will present a remarkable vibration if the frequency is higher than 45 Hz, which will in return lower the weld quality and service time of the machine.

### 3.3. Effect of amplitude of oscillation

Wanjara and Jahazi [8] reported that the welding time decreased with increasing amplitude under constant frequency and

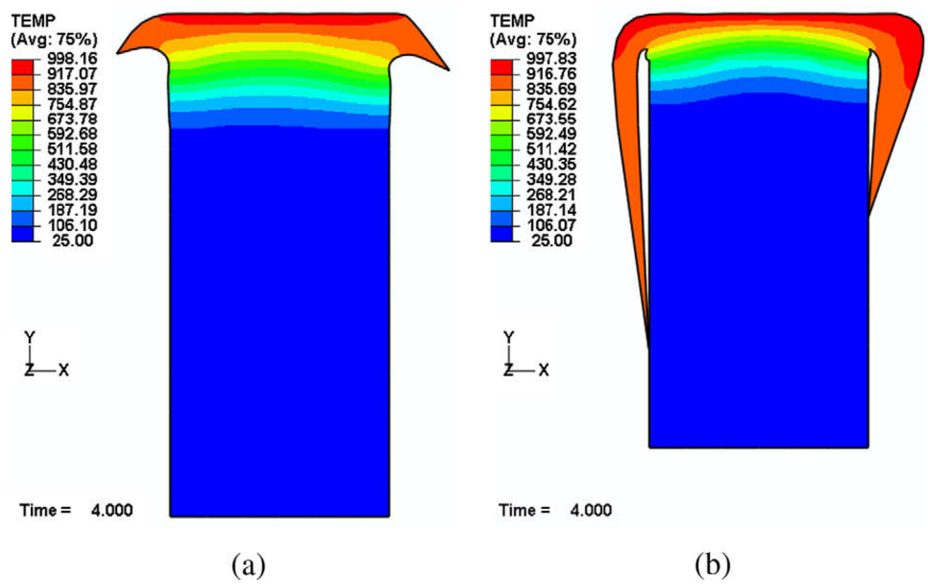


**Fig. 12.** Temperature contours in the specimens obtained under different oscillation frequencies at the friction time of 4 s. (a) 25 Hz and (b) 45 Hz.

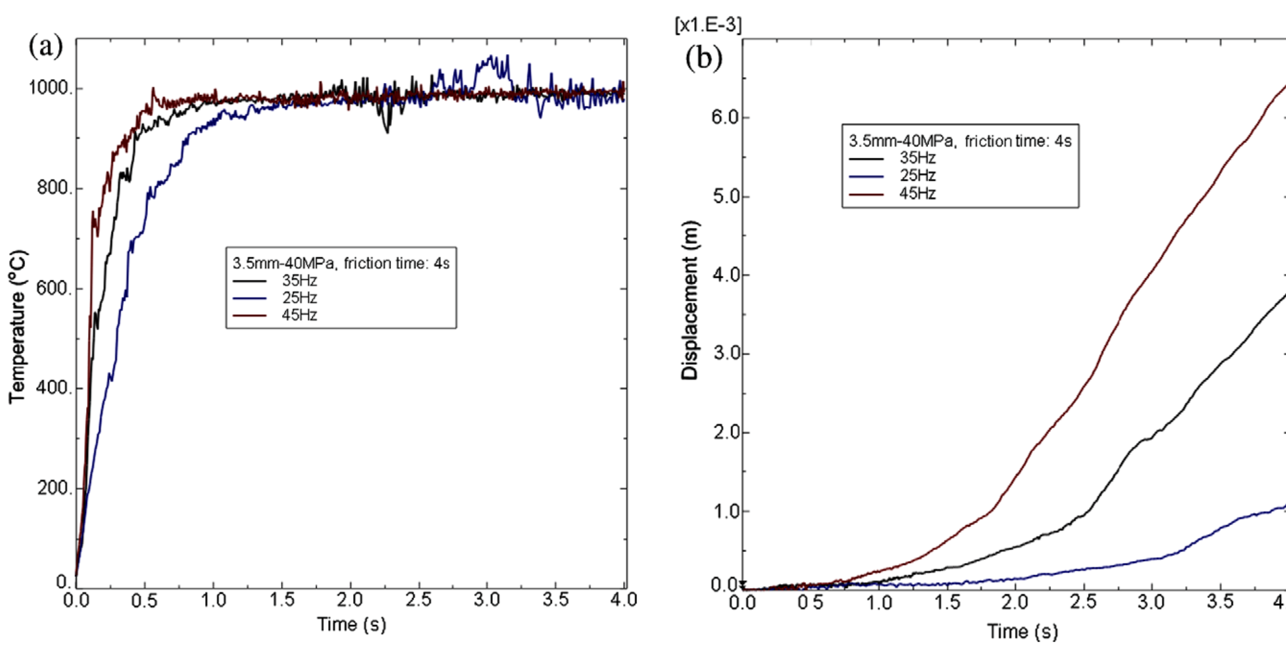


**Fig. 13.** Changes of temperature of the central element at the interface (a) and unilateral axial shortening (b) with the friction time obtained under different oscillation frequencies.

axial pressure. One may expect that the increase of amplitude will increase the total frictional heat. Based on the results in Section 3.1, the oscillation amplitude is changed to 2.5 mm and 4.5 mm from 3.5 mm with the same frequency of 35 Hz and friction pressure of 40 MPa. The simulated results are shown in Figs. 14 and 15. Compared to the results obtained under the amplitude of 3.5 mm (Fig. 6d), the case of amplitude 2.5 mm (Fig. 14a) presents a worse results. Similar to the situation of low frequency, although the interface temperature reaches 1000 °C at 1.5 s, a little flash is formed at 4 s (Fig. 14a) and the total unilateral axial shortening is about 1.3 mm (Fig. 15b). Similarly, the uniformly distributed high interface temperature could not be obtained in earlier stage of the process under the amplitude of 2.5 mm. Under this situation, an appropriate temperature field could not be formed even at 4 s. Thus, a long friction time is needed due to the low heat input. Although this disadvantage could be compromised with a high frequency or pressure [1,8], the exposed interface may be oxidized during the process.

When the amplitude is 4.5 mm, the unilateral axial shortening is about 4.6 mm at 3 s (Fig. 15b). Much more materials have been extruded to form the flash (Fig. 14b) than the 2.5 mm case. Excessive distortion of some elements in the model terminated the program prematurely at about 3.2 s. The axial shortening is expected to be 6 mm or more at 4 s from a linear extrapolation. The interface temperature with the amplitude of 4.5 mm increased rapidly to about 1000 °C at 0.5 s (Fig. 15a). The interface temperature becomes uniform across the interface earlier compared to the 2.5 mm case. In addition, compared to that with 2.5 mm ampli-

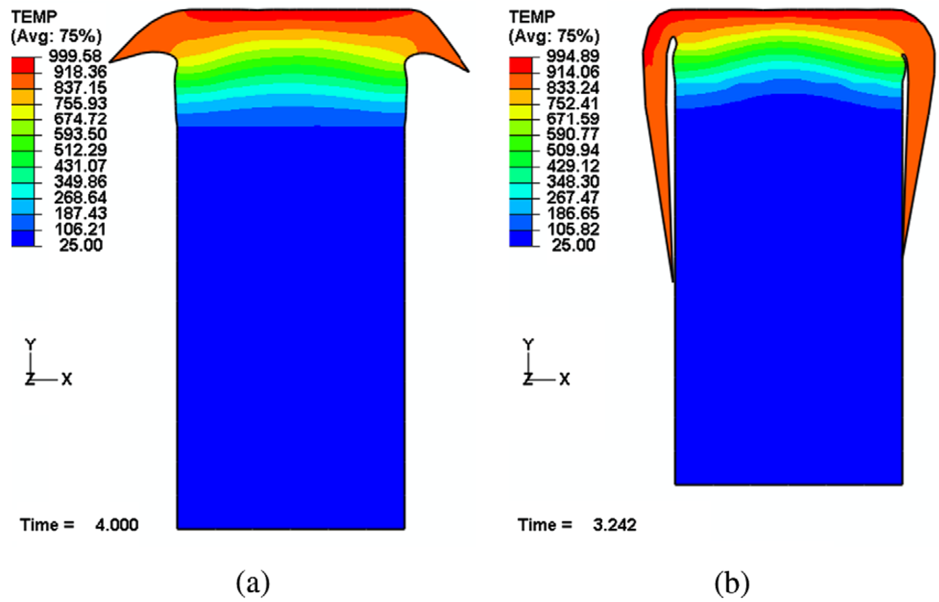


**Fig. 14.** Temperature contours in the specimens obtained under different amplitudes. (a) 2.5 mm, friction time of 4 s; (b) 4.5 mm, friction time of 3.242 s.

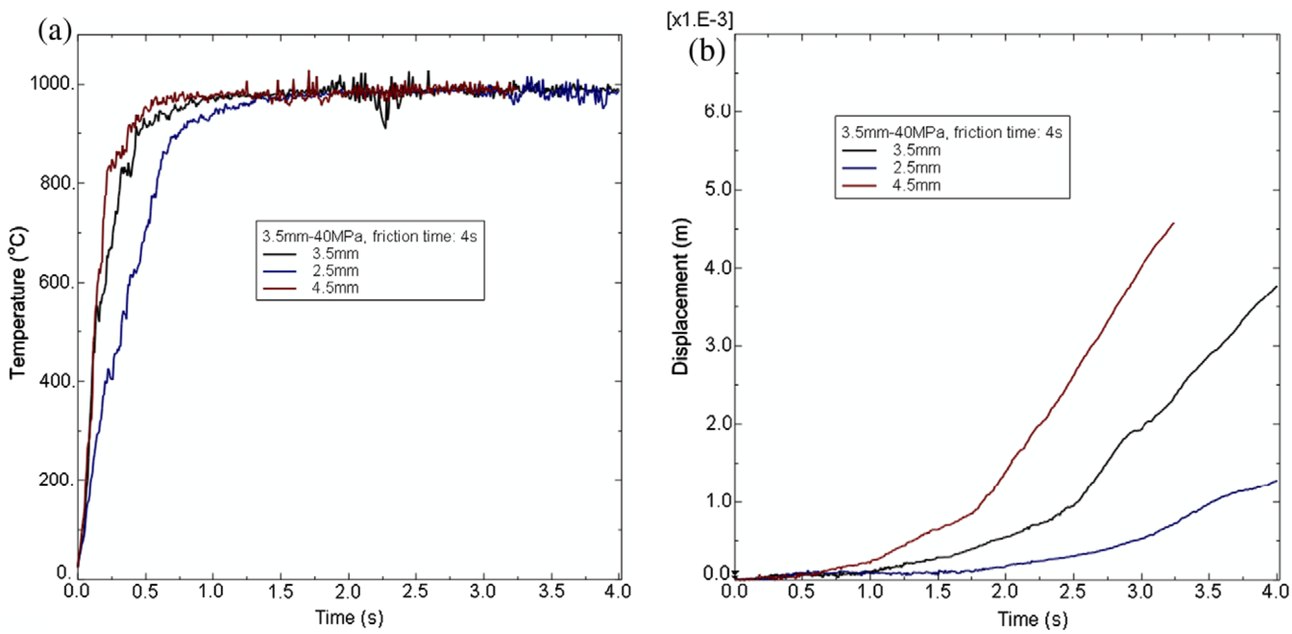


**Fig. 15.** Changes of temperature of the central element at the interface (a) and unilateral axial shortening (b) with the friction time obtained under different amplitudes.

tude, the high temperature zone is more limited in the interface zone because of the faster extrusion of plasticized materials.

Similarly, the fast deformation rate (Fig. 15b) may be unfavorable to precision control. Moreover, an important concern is the oxidation of the interface because the larger vibration exposes the high temperature metal for a longer time. In addition, the larger amplitude also increases the difficulty in the alignment of the joint. Therefore, an appropriate amplitude is necessary, which is usually less than 4 mm [1,8].

### 3.4. Effect of friction pressure

As reported, the increase of pressure could increase the power input [1,8] and reduce the welding time [8]. In this study, besides 40 MPa, the friction pressure is changed to 20 MPa and 60 MPa with the constant frequency of 35 Hz and amplitude of 3.5 mm.

The calculated results for the case of 20 MPa are given in Figs. 16 and 17. Compared to the results obtained under 40 MPa (Fig. 6d), the interface temperature reached 1000 °C at about 3 s (Fig. 17a). However, the interface temperature is not uniform (Fig. 16a). It is found that the interface temperature increased relatively slower and the margin temperature is too low to obtain an appropriate temperature field. The entire unilateral axial shortening is only 0.1 mm and almost no flash is formed. This means that the deformation rate is relatively slow owing to the lower heat input. In practice, it is very difficult to form a sound weld under this condition even if the friction time could be long.

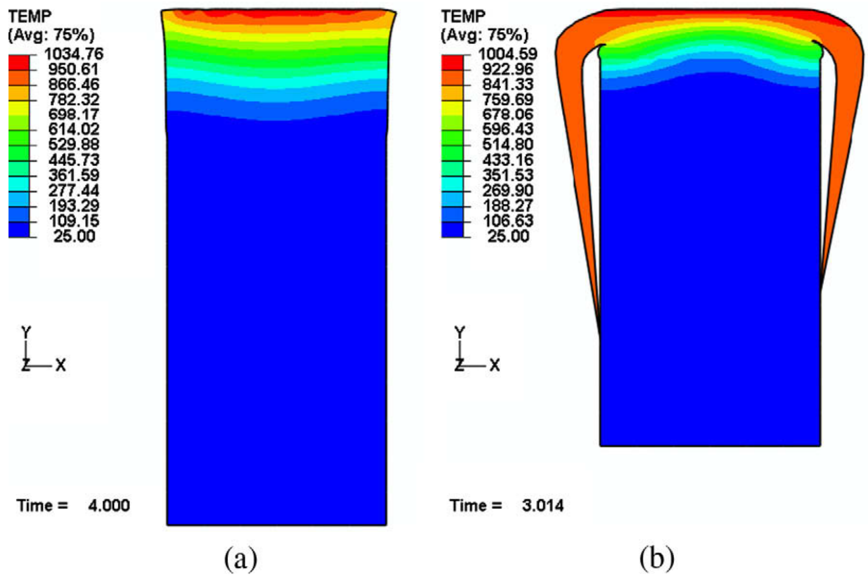


**Fig. 16.** Temperature contours in the specimens obtained under different friction pressures. (a) 20 MPa, friction time of 4 s; (b) 60 MPa, friction time of 3.014 s.

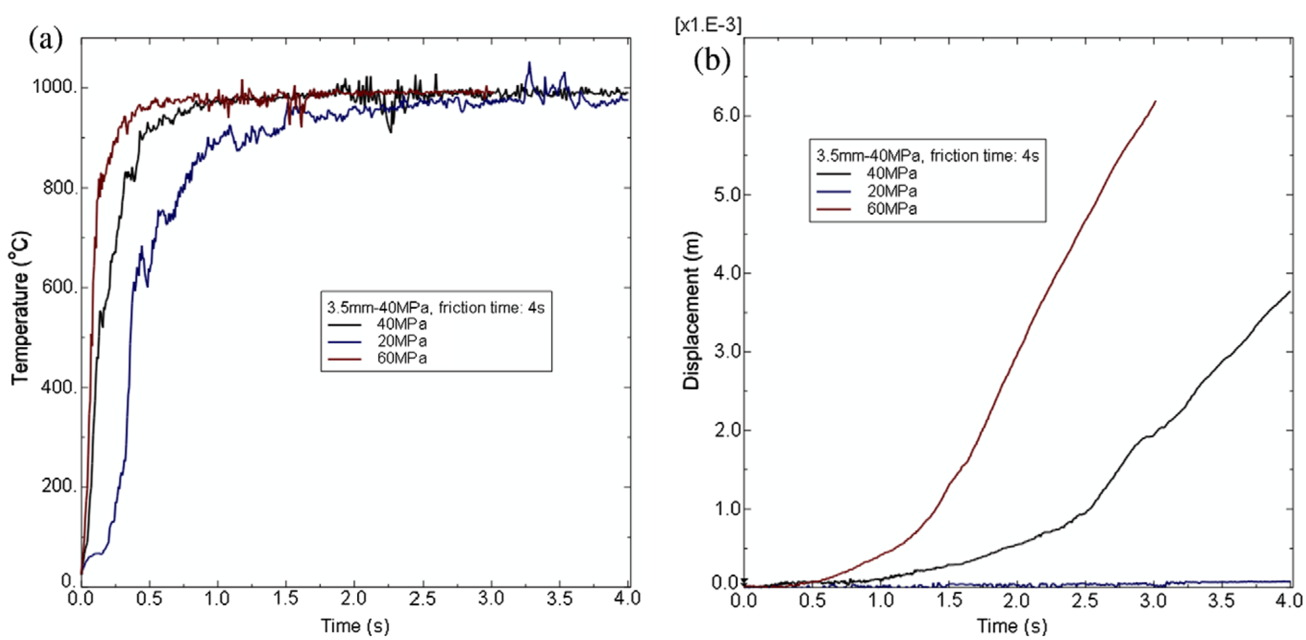


**Fig. 17.** Changes of temperature of the central element at the interface (a) and unilateral axial shortening (b) with the friction time obtained under different friction pressures.

As the friction pressure is increased to 60 MPa, the interface temperature can increase more rapidly to about 1000 °C within 0.5 s (Fig. 17a). At 3 s, the unilateral axial shortening is increased to about 6.2 mm at a faster rate (Fig. 17b). But the program was terminated at 3 s owing to the excessive distortion of some elements. The estimated axial shortening could be about 8 mm or more at 4 s from a linear extrapolation. The interface temperature under 60 MPa is more uniform with the obvious flash at 4 s (Fig. 16b).

Although higher pressure may generate larger high-temperature interface zone (Fig. 16b), a larger interface grain size would be formed due to the excessive heat input at the interface [8]. On the other hand, positive increase in friction pressure appears to have a small negative effect on weld quality as measured by the Charpy impact test [1]. In addition, a high pressure will cause a remarkable elastic deformation of the champing device of the machine, and in return, lower the precision of alignment and the joint quality. The obvious deformation of jig was observed in the experiments with the machine of our university under high pressure process. Therefore, careful selection of the pressure should also be exercised.

## 4. Discussion on the effects of different factors

According to the above results, it is found that those three factors, i.e., oscillation frequency, amplitude and friction pressure are not independent, which are interactional as suggested by Vairis and Frost [1], Wanjara and Jahazi [8]. Through correlation with the processing parameters, microstructure and properties of LFW

TC4 joints, Wanjara and Jahazi [8] outlined the critical processing conditions, e.g. a frequency of 50 Hz, an amplitude of 2 mm, a pressure of 50 MPa, and a shortening of 2 mm which can offer both high quality and reliability as well as excellent tensile properties that can surpass that of the parent TC4. The relative effects of the frequency, amplitude and pressure on the welding time can be reasoned on the basis of the power input required for reaching critical strain and temperature conditions at the welding interface [8].

Based on our previous analysis [12], the average heat input (*HI*) during LFW for the developed machine can be simply characterized as follows:

$$HI = 4\mu fAP \tag{3}$$

where $\mu$ is the average friction coefficient, $f$ and $A$ are respectively the oscillation frequency and amplitude, $P$ is the friction force (friction pressure times sectional area). Eq. (3) shows that the heat input is proportional to the oscillation frequency, amplitude and friction pressure. The higher frequency, amplitude and pressure will inevitably generate more heat at the interface, and thus a faster increase of interface temperature and deformation rate. Consequently, taking the average friction coefficient as 0.6 [3,18], the average heat inputs under different combinations of processing parameters in this study are calculated and plotted against the unilateral axial shortening as shown in Fig. 18. It is interesting to see that the axial shortening is almost linearly with the heat input when the heat input is higher than a critical value. It could be argued that this critical value is influenced by the properties of the materials to be welded. As previously reported by Vairis and Frost [1], for TC4 titanium alloy, the minimum heat input for a successful weld was about $0.75 \times 10^7$ W/m$^2$ and it should be larger than $1.5 \times 10^7$ W/m$^2$ for a joint of good-quality. This is in good agreement with the results obtained in this study (Fig. 18). Accordingly, the appropriate heat input for our case appears to be in the range of $1.2 \times 10^7$–$1.5 \times 10^7$ W/m$^2$. Based on the tensile properties of the welded joints, Wanjara and Jahazi [8] also indicated the heat input for a sound weld (without welding defects such as centerline porosity or oxides) should be higher than 2.4 kW under their welding conditions.

On the other hand, the minimum heat input required to achieve welding conditions was found to be a little dependent on the oscillation frequency and amplitude [1]. That means an appropriate combination of processing parameters is necessary to obtain a sound weld. According to the results obtained in this study, it is concluded that the frequency of 35 Hz, amplitude of 3.5 mm and pressure of 40 MPa is a combination for LFW TC4. These are consistent with our previous experiments with similar heat input [9]. It is also concluded that one can optimize the LFW processing parameters through the simulation model such as the current analysis provided the parent material's properties are known. However, Wanjara and Jahazi [8] also concluded that the power input could not be used alone as an exclusive criterion for defining weld integrity. The axial shortening condition should also be included as a necessary parameter for the LFW process. Nevertheless, it is anticipated that numerical simulation can be helpful in developing the controls of a LFW process and the weld quality with less experimental work and therefore saving cost.

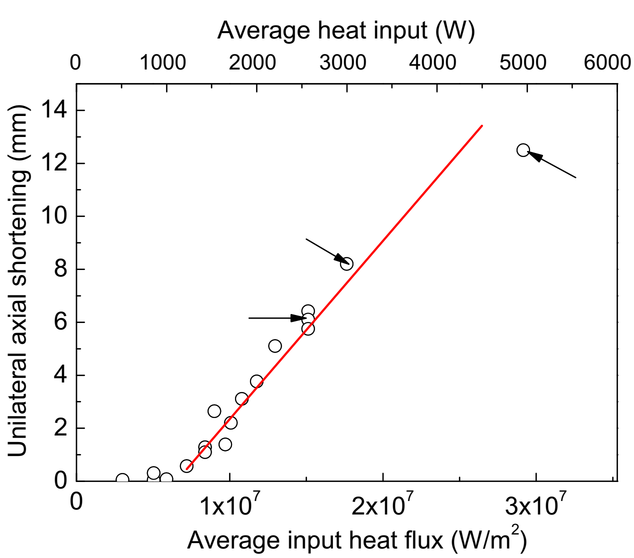


**Fig. 18.** Relationship between average heat input and axial shortening. Note the shortening values indicated by the arrows are estimated from a linear extrapolation because of the abnormal termination of the program.

Finally, at the presence of a quasi-steady state during LFW, the processing parameters (or the integrated factor: heat input) have little effect on the interface temperature, the thicknesses of the high temperature zone and the HAZ given a weld is successfully obtained.

## 5. Conclusions

Numerical modeling of linear friction welding (LFW) of TC4 titanium alloy by a combination of explicit and implicit finite element analysis was conducted. Based on the investigation on the effects of processing parameters on the temperature evolution and axial shortening of specimen, the following conclusions could be made.

(1) The interface temperature can increase quickly to higher than 1000 °C within 1 s under certain processing conditions. But the interface temperature at the margin is much lower and no obvious axial shortening is formed at the initial stage. After that, the interface temperature increased slowly and tends to be uniform across the interface, which causes significant increase of axial shortening and fast extrusion of flash. During the cooling process, the interface temperature decreased steeply at a speed of several hundreds degrees per second because of the heat conduction to the cold end of specimen. The temperature distribution tends to be uniform in the joint after about 30 s. In addition, the temperature gradient across the joint from the interface is very large during the process. The thermal history in the joint developed through the LFW process will eventually influence the joint microstructure and properties.

(2) As the oscillation frequency increases, the interface temperature reaches more quickly up to a high temperature and the axial shortening also increases to a larger value at a faster rate. The same holds for the increases of both amplitude and friction pressure. The effects of these three factors are not independent, which can be integrated into one factor of heat input. The heat input is linearly proportional to the oscillation frequency, amplitude and friction pressure. If the heat input is higher than a critical value, the axial shortening would increase nearly linearly with increasing heat input. In conclusion, an appropriate heat input, i.e., proper combination of these three factors, is necessary to achieve a sound weld.

## Acknowledgements

The authors would like to thank the financial support from the Aoxiang Star Project of NPU. The project was also sponsored by the Scientific Research Foundation for the Returned Overseas Chinese Scholars, State Education Ministry, and the Program for New Century Excellent Talents in University by the Ministry of Education of the People's Republic of China. Finally, the authors thank Professor Bill Y.J. Chao from Mechanical Engineering, University of South Carolina, USA for the help in polishing grammar.

## References

[1] Vairis A, Frost M. High frequency linear friction welding of a titanium alloy. Wear 1998;217:117–31.
[2] Vairis A, Frost M. On the extrusion stage of linear friction welding of Ti 6Al 4V. Mater Sci Eng A 1999;271:477–84.
[3] Vairis A, Frost M. Modelling the linear friction welding of titanium blocks. Mater Sci Eng A 2000;292:8–17.
[4] Bußmann M, Bayer E. Market-oriented blisk manufacturing: a challenge for production engineering. p. 12–13 <http://www.mtu.de/de/technologies/engineering_news/bayer_bliskfertigung.pdf> [accessed 2008].
[5] Corzo M, Torres Y, Anglada M, Mateo A. Fracture behaviour of linear friction welds in titanium alloys. Anal Mec Fract 2007;1:75–80.
[6] Roder O, Ferte J-P, Gach E, Mendez J, Anglada M, Mateo A. Development and Validation of a dual titanium alloy dual microstructure BLISK. In: Fifth aeronautic days 2006, Vienna, Austria; June 19th–21st 2006.
[7] Baeslack III WA, Broderick TF, Juhas M, Fraser HL. Characterization of solid-phase welds between Ti–6Al–2Sn–4Zr–2Mo–0.1Si and Ti13.5Al–21.5Nb titanium aluminide. Mater Charac 1994;33:357–67.
[8] Wanjara P, Jahazi M. Linear friction welding of Ti–6Al–4V: processing, microstructure, and mechanical-property inter-relationships. Metall Mater Trans A 2005;36:2149–64.
[9] Li WY, Ma TJ, Zhang Y, Xu QZ, Li JL, Yang SQ, Liao HL. Microstructure characterization and mechanical properties of linear friction welded Ti–6Al–4V alloy. Adv Eng Mater 2008;10:89–92.
[10] Karadge M, Preuss M, Lovell C, Withers PJ, Bray S. Texture development in Ti–6Al–4V linear friction welds. Mater Sci Eng A 2007;459:182–91.
[11] Karadge M, Preuss M, Withers PJ, Bray S. Importance of crystal orientation in linear friction joining of single crystal to polycrystalline nickel-based superalloys. Mater Sci Eng A 2008;491:446–53.
[12] Li WY, Ma TJ, Xu QZ, Yang SQ, Zhang Y, Li JL, Liao HL. Effect of friction time on flash shape and axial shortening of linear friction welded 45 steel. Mater Lett 2008;62:293–6.
[13] Ma TJ, Li WY, Xu QZ, Zhang Y, Li JL, Yang SQ, Liao HL. Microstructure evolution and mechanical properties of linear friction welded 45 steel joint. Adv Eng Mater 2007;9:703–7.
[14] Threadgill P. Linear friction welding. TWI knowledge summary. The Welding Institute, UK. <http://eurostir.co.uk/j32k/protected/band_3/ksplt001.html> [accessed 2008-10-10].
[15] Ma TJ, Li WY, Yang SQ. Impact toughness and fracture analysis of linear friction welded Ti–6Al–4V alloy joints. Mater Des 2009;30:2128–32.
[16] Tao J, Zhang TC, Liu P, Li J, Mang Y. Numerical computation of a linear friction welding process. Mater Sci Forum 2008;575–578:811–5.
[17] ABAQUS analysis user's manual, ABAQUS Version 6.7 HTML documentation. Dassault Systèmes; 2007.
[18] Vairis A. Investigation of frictional behaviour of various materials under sliding conditions. Eur J Mech A 1997;16:929–45.
[19] Meyers MA. Dynamic behavior of materials. New York: John Wiley & Sons Inc.; 1994.
[20] Boyer R, Welsch G, Collings EW. Materials properties handbook: titanium alloys. Weinkeim, Germany: Willey-VCH GmbH & Co KGaA; 1994.
[21] Huang BY, Li CG, Shi LK, Qiu GZ, Zuo TY. China materials engineering canon. Nonferrous materials and engineering (part 1), vol. 4. Beijing: Chemical Industry Press; 2006 [in Chinese].
[22] Daridon L, Oussouaddi O, Ahzi S. Influence of the material constitutive models on the adiabatic shear band spacing: MTS, power law and Johnson–Cook model. Int J Solids Struct 2004;41:3109–24.
[23] Chaudhury P, Zhao D. Atlas of formability: Ti 6Al 4V ELI. Technical report. National Center for Excellence in Metalworking Technology; 1992.
[24] Yang HQ. Finite element simulation of residual stresses and distortions during the welding of a pipe. In: AIAA/ASME/ASCE/AHS/ASC structures, structural dynamics, and materials conference, 32nd, Baltimore, MD, April 8–10, 1991, Technical Papers. Pt. 2 (A91-31826 12-39). Washington, DC: American Institute of Aeronautics and Astronautics; 1991. p. 1402–12.